International Journal of Innovative Computing, Information and Control
Volume **8**, Number **5(A)**, May **2012**

ICIC International ©2012 ISSN 1349-4198
pp. 3411–3429

FPGA-BASED ROBUST ADAPTIVE CONTROL OF BLDC MOTORS USING FUZZY CEREBELLAR MODAL ARTICULATION CONTROLLER

Chih-Min Lin[1,*], Ang-Bung Ting[1], Chun-Fei Hsu[2] and Chao-Ming Chung[3]

[1]Department of Electrical Engineering
Yuan Ze University
No. 135, Yuan-Dong Rd., Chung-Li, Tao-Yuan 320, Taiwan
*Corresponding author: cml@saturn.yzu.edu.tw; s968501@mail.yzu.edu.tw

[2]Department of Electrical Engineering
Tamkang University
No. 151, Yingzhuan Rd., Tamsui Dist., New Taipei City 251, Taiwan
fei@ee.tku.edu.tw

[3]Chung Shan Institute of Science and Technology
P.O. Box 90008-15, Lung-Tan, Tao-Yuan 325, Taiwan
chaoming@saturn.yzu.edu.tw

Received February 2011; revised June 2011

Abstract. *A novel fuzzy cerebellar-model-articulation-controller (CMAC), which is a generalization of a fuzzy neural-network, is developed in this study. Moreover, this paper proposes a robust adaptive control (RAC) system for brushless DC (BLDC) motors using a fuzzy CMAC (FCMAC). The proposed RAC system is composed of an FCMAC and a robust controller. The FCMAC is developed to serve as the main controller and the robust controller is designed to attenuate the effect of the approximation error between the FCMAC and an ideal controller. The developed RAC system is implemented in a field programmable gate array (FPGA) chip to control a BLDC motor in a real-time mode. Using an FPGA to implement an FCMAC for real-time control systems is also a novel approach. For comparison, an adaptive CMAC-based supervisory control, a robust adaptive fuzzy control and the proposed RAC are employed to control a BLDC motor. The experimental results verify that the proposed RAC can achieve better tracking performance than the other control methods.*

Keywords: Adaptive control, Robust control, Fuzzy system, Cerebellar model articulation controller, Brushless DC motor, Field programmable gate array

1. **Introduction.** According to the approximation property of neural network (NN), the NN-based adaptive controllers have been developed to compensate for the effects of nonlinearities and system uncertainties [1-4]. In order to obtain fast learning property and good generalization ability, cerebellar model articulation controller (CMAC) has been proposed [5-7]. CMAC is classified as a non-fully connected perceptron-like associative memory network with overlapping receptive fields, and it intends to resolve the fast size-growing problem in the currently available types of neural networks (NNs). It has already been validated that CMAC can approximate a nonlinear function over a domain of interest to any desired accuracy. There has recently been considerable interest in exploring the applications of CMAC to deal with the uncertainty and nonlinearity of control systems [6,8]. It has been shown, in some cases, that CMAC-based control systems can achieve better control performance than NN-based control systems [9,10]. Moreover, to accommodate the fuzziness of input data, the structure of CMAC with input fuzzification

has been proposed in recent years [10-13]. However, in these studies, only the fuzziness of input data is considered; and for these CMACs, the membership functions in each block are binary. This structure will constrain the approximation accuracy of the CMAC. Moreover, these CMACs are not related to any fuzzy rule base. Furthermore, the conventional CMAC-based control systems used an integral learning algorithm [6-12]. Thus, the convergence of the controller's parameters and tracking errors may be slow. In this study, a novel CMAC-based fuzzy rule system is proposed to obtain the fast learning property and good generalization ability. This fuzzy CMAC (FCMAC) is a generalization of a fuzzy neural network. Moreover, a PI-learning algorithm of the controller's parameters is developed to speed up the learning process.

The brushless DC (BLDC) motor has the advantages of simple structure, high torque, small inertia, low noise and long life operation [14,15]. Hence, it has gradually been used in the motion control applications such as electric vehicles, aeronautics, robotics, dynamic actuation and micro electric motor cars. In recent years, several investigations have been carried out by applying various control algorithms to control the BLDC motors [16-18]. Rubaai et al. proposed an adaptive fuzzy-neural-network controller to achieve satisfactory tracking performance with unknown motor dynamics [16]. However, the convergent speed is too slow and the computation load is heavy. Li and Xia proposed a computation controller with a CMAC and a PID controller to improve the control precision [17]. However, the learning algorithm is developed from the gradient descent method; thus, the system stability cannot be guaranteed. Rubaai and others proposed a robust adaptive fuzzy controller to achieve tracking performance with desired attenuation level [18]. However, this approach only tunes the parameters of the consequence part of the fuzzy rules. The parameters of the antecedent part should be constructed by trial-and-error.

This paper proposes a robust adaptive control (RAC) system to control a BLDC motor. The RAC system is composed of an FCMAC and a robust controller. The proposed PI learning FCMAC is used as the main controller to mimic an ideal controller, and the robust controller is designed to achieve L_2 robust tracking performance with desired attenuation level. Then, the proposed control system is implemented on an Altera Stratix II series field programmable gate array (FPGA) chip to achieve low-cost, high-performance industrial applications. A characteristic comparison among an adaptive CMAC-based supervisory control [6], a robust adaptive fuzzy control [19] and the proposed RAC is made to illustrate the effectiveness of the proposed control method.

2. **Formulation of BLDC Motor Control System.** The system equations of BLDC motor driver in a d-q model can be expressed as [18]

$$\dot{i}_{qs} = -\frac{R_s}{L_q} i_{qs} - \frac{L_d}{L_q} \omega_r i_{ds} + \frac{1}{L_q} V_{qs} - \frac{\lambda_m}{L_q} \omega_r \tag{1}$$

$$\dot{i}_{ds} = -\frac{R_s}{L_d} i_{ds} + \frac{L_q}{L_d} \omega_r i_{qs} + \frac{1}{L_d} V_{ds} \tag{2}$$

$$L_q = L_{is} + L_{mq} \tag{3}$$

$$L_d = L_{is} + L_{md} \tag{4}$$

and the torque equation is expressed as

$$T_e = \frac{3}{2}\frac{N}{2}[\lambda_m i_{qs} + (L_d - L_q) i_{qs} i_{ds}] \tag{5}$$

where R_s is the stator resistance, L_{is} is the stator leakage inductance, ω_r is the electrical rotor angular velocity, λ_m is the flux linkage of the permanent magnet, N is the number of poles, and i_{ds} and i_{qs} are the stator currents, L_d and L_q are the stator inductances,

V_{ds} and V_{qs} are the stator voltages, L_{md} and L_{mq} are the magnetizing inductances of the d and q axes, respectively. Considering the mechanical load, the dynamic equation of BLDC motor can be written as

$$J\frac{2}{N}\dot{\omega}_r + B\frac{2}{N}\omega_r = T_e - T_L \tag{6}$$

where J is the inertia of the system, B is the damping coefficient, and T_L is the load disturbance. By using the field-oriented control, it can make i_{ds} become zero. Therefore, the equation of BLDC motor driver can be rewritten as [20]

$$\dot{i}_{qs} = -\frac{R_s}{L_q}i_{qs} + \frac{1}{L_q}V_{qs} - \frac{\lambda_m}{L_q}\omega_r \tag{7}$$

$$\dot{\omega}_r = \frac{3}{2}\frac{1}{J}\left(\frac{N}{2}\right)^2 \lambda_m i_{qs} - \frac{B}{J}\omega_r - \frac{N}{2J}T_L \tag{8}$$

and the torque equation is expressed as

$$T_e = \frac{3}{2}\frac{N}{2}\lambda_m i_{qs} = k_t i_{qs} \tag{9}$$

where $k_t = \dfrac{3}{2}\dfrac{N}{2}\lambda_m$ is the constant gain. From (9), the dynamic Equation (8) can be rewritten as

$$\ddot{\theta} = f\dot{\theta} + gu + h \tag{10}$$

where $\theta = \int \omega_r dt$ is the position of the rotor, $f = -\dfrac{B}{J}$, $g = \dfrac{N}{2}\dfrac{k_t}{J}$, $h = -\dfrac{N}{2J}T_L$, and $u = i_{qs}$. It can be seen that f and g are constants. The control objective is to find a control law so that the rotor position θ can closely track the position command θ_c. Define the tracking error as

$$e = \theta_c - \theta. \tag{11}$$

Assume the parameters of the controlled system in (10) are well known, there exists an ideal controller

$$u^* = g^{-1}(-f\dot{\theta} - h + \ddot{\theta}_c + k_1\dot{e} + k_2 e) \tag{12}$$

where k_1 and k_2 are positive constants. Applying the ideal controller (12) into (10) yields the following error dynamics

$$\dot{\mathbf{e}} = \mathbf{\Lambda}\mathbf{e} \tag{13}$$

where $\mathbf{e} = [e \ \dot{e}]^T$, and $\mathbf{\Lambda} = \begin{bmatrix} 0 & 1 \\ -k_2 & -k_1 \end{bmatrix}$. By the adequate choice of k_1 and k_2, $\mathbf{\Lambda}$ can be a Hurwitz matrix, it implies $\lim\limits_{t\to\infty} e = 0$ for any starting initial conditions. Since the system dynamics f and g, and the disturbance h may be unknown or perturbed in practical applications, the ideal controller u^* in (12) cannot be precisely obtained. Thus, an FCMAC will be designed to approximate the ideal controller.

3. **FCMAC Approximator.** A novel FCMAC is proposed with the following fuzzy inference rules:

$$\begin{aligned} R^\lambda: \ &\text{If } I_1 \text{ is } \varphi_{1jk} \text{ and } I_2 \text{ is } \varphi_{2jk}, \cdots, \ I_{n_i} \text{ is } \varphi_{n_i jk} \text{ then } y_{jk} = w_{jk} \\ &\text{for } j = 1, 2, \cdots, n_j, \ k = 1, 2, \cdots, n_k, \text{ and } \lambda = 1, 2, \cdots, n_l \end{aligned} \tag{14}$$

where n_i is the input dimension, n_j is the number of layers for each input dimension, n_k is the number of blocks for each layer, n_l is the number of fuzzy rules, φ_{ijk} is the fuzzy set for the ith input, jth layer and kth block, and w_{jk} is the output weight in the consequent part. Contrary to the fuzzy neural network, this FCMAC possesses the structure with layers and blocks in the input space. In this FCMAC, if every block is chosen to contain only one

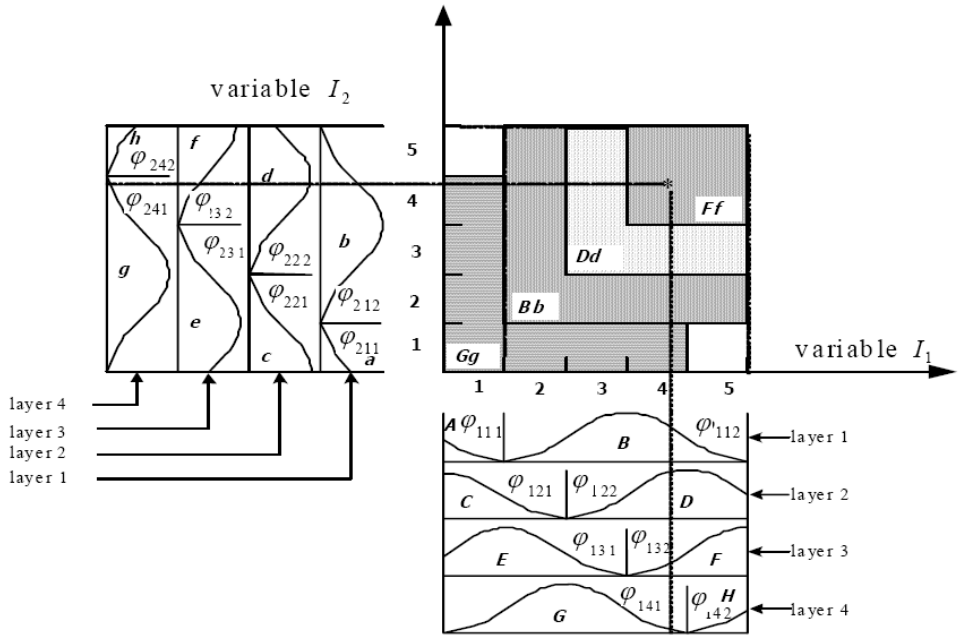

FIGURE 1. A two-dimensional fuzzy CMAC

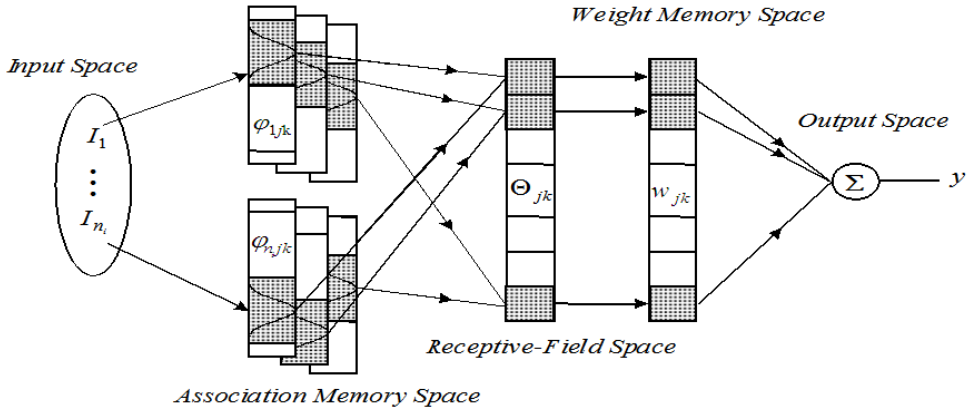

FIGURE 2. The architecture of a fuzzy CMAC

element (neuron) and there is only one layer for each input space, then this FCMAC can be reduced to a fuzzy neural network. Thus, this FCMAC can be viewed as a generalization of a fuzzy neural network and it presents better generalization capability, fast leaning property and quick recalling ability than the fuzzy neural network. A schematic diagram of a two-dimensional ($n_i = 2$) FCMAC with four layers ($n_j = 4$) and two blocks ($n_k = 2$) in each layer is depicted in Figure 1.

An FCMAC is proposed and shown in Figure 2. The receptive-field basis function and the signal propagation in each space are described as follows.

1) *Input*: For a given $\mathbf{I} = [I_1, \cdots, I_i, \cdots, I_{n_i}]^T \in \Re^{n_i}$, where n_i is the number of input state variables, each input state variable I_i can be quantized into discrete regions (called elements or neurons) according to given control space. The number of elements, n_e, is termed as a resolution.

2) *Association memory (Membership function)*: Several elements can be accumulated as a block. In this space, each block performs a receptive-field basis function. The Gaussian

function is adopted as the receptive-field basis function which can be represented as

$$\varphi_{ijk}(I_i) = \exp\left[\frac{-(I_i - m_{ijk})^2}{\sigma_{ijk}^2}\right], \text{ for } i = 1, 2, \cdots, n_i,\ j = 1, 2, \cdots, n_j, \text{ and } k = 1, 2, \cdots, n_k \tag{15}$$

where $\varphi_{ijk}(I_i)$ presents the receptive-field basis function for the jth layer and kth block of the ith input I_i with the mean m_{ijk} and variance σ_{ijk}.

3) *Receptive-field*: Each block has two adjustable parameters, mean m_{ijk} and variance σ_{ijk}. The multi-dimensional receptive-field function is defined as

$$\Theta_{jk} = \prod_{i=1}^{n_i} \phi_{ijk} \quad \text{for } j = 1, 2, \cdots, n_j, \text{ and } k = 1, 2, \cdots, n_k \tag{16}$$

where Θ_{jk} is associated with the jth layer and kth block; i.e., in the fuzzy rules in (14), the product is used as the "and" computation in the antecedent part.

The multi-dimensional receptive-field functions can be expressed in a vector form as

$$\boldsymbol{\Theta} = [\Theta_{11},\ \cdots,\ \Theta_{1n_k},\ \Theta_{21},\ \cdots,\ \Theta_{2n_k},\ \cdots,\ \Theta_{n_j1},\ \cdots,\ \Theta_{n_jn_k}]^T \in \Re^{n_j n_k} \tag{17}$$

4) *Weight memory (Fuzzy output weight)*: Each location of receptive-field to a particular adjustable value in the weight memory space can be expressed as

$$\mathbf{w} = [w_{11},\ \cdots,\ w_{1n_k},\ w_{21},\ \cdots,\ w_{2n_k},\ \cdots,\ w_{n_j1},\ \cdots,\ w_{n_jn_k}]^T \in \Re^{n_j n_k} \tag{18}$$

where w_{jk} denotes the connecting weight value of the output associated with the jth layer and kth block. This means that a singleton value w_{jk} is chosen as the consequent part in the fuzzy rules in (14).

5) *Output (Defuzzification)*: The output of FCMAC is the algebraic sum of the activated weighted receptive-field, and is expressed as

$$u_{FCMAC} = y = \mathbf{w}^T \boldsymbol{\Theta}(\mathbf{I}, \mathbf{m}, \boldsymbol{\sigma}) = \sum_{j=1}^{n_j} \sum_{k=1}^{n_k} w_{jk} \Theta_{jk} \tag{19}$$

where

$$\mathbf{m} = \left[m_{111}, \ldots, m_{n_i11}, \cdots, m_{1n_j1}, \ldots, m_{n_in_j1}, \ldots, m_{1n_jn_k}, \ldots, m_{n_in_jn_k}\right]^T \in \Re^{n_i n_j n_k} \tag{20}$$

$$\boldsymbol{\sigma} = \left[\sigma_{111}, \ldots, \sigma_{n_i11}, \cdots, \sigma_{1n_j1}, \ldots, \sigma_{n_in_j1}, \ldots, \sigma_{1n_jn_k}, \ldots, \sigma_{n_in_jn_k}\right]^T \in \Re^{n_i n_j n_k} \tag{21}$$

This implies the existence of an FCMAC of (19) that can uniformly approximate the ideal controller u^* [21]. Assume that exists an optimal FCMAC such that

$$u^* = u^*_{FCMAC} + \Delta = \mathbf{w}^{*T} \boldsymbol{\Theta}(\mathbf{I}, \mathbf{m}^*, \boldsymbol{\sigma}^*) + \Delta = \mathbf{w}^{*T} \boldsymbol{\Theta}^* + \Delta \tag{22}$$

where Δ denotes the approximation error, $\mathbf{w}^*$ and $\boldsymbol{\Theta}^*$ are the optimal parameter vectors of $\mathbf{w}$ and $\boldsymbol{\Theta}$, respectively, and $\mathbf{m}^*$ and $\boldsymbol{\sigma}^*$ are the optimal parameter vectors of $\mathbf{m}$ and $\boldsymbol{\sigma}$, respectively. In fact, the optimal parameter vectors needed to best approximate u^* cannot be determined. Thus, an estimation function is defined as

$$\hat{u}_{FCMAC} = \hat{\mathbf{w}}^T \boldsymbol{\Theta}(\mathbf{I}, \hat{\mathbf{m}}, \hat{\boldsymbol{\sigma}}) = \hat{\mathbf{w}}^T \hat{\boldsymbol{\Theta}} \tag{23}$$

where $\hat{\mathbf{w}}$ and $\hat{\boldsymbol{\Theta}}$ are the estimated parameter vectors of $\mathbf{w}$ and $\boldsymbol{\Theta}$, respectively, and $\hat{\mathbf{m}}$ and $\hat{\boldsymbol{\sigma}}$ are the estimated parameter vectors of $\mathbf{m}$ and $\boldsymbol{\sigma}$, respectively. Define the estimation error as

$$\tilde{u}_{FCMAC} = u^* - \hat{u}_{FCMAC} = \mathbf{w}^{*T} \boldsymbol{\Theta}^* - \hat{\mathbf{w}}^T \hat{\boldsymbol{\Theta}} + \Delta = \tilde{\mathbf{w}}^T \tilde{\boldsymbol{\Theta}} + \hat{\mathbf{w}}^T \tilde{\boldsymbol{\Theta}} + \tilde{\mathbf{w}}^T \hat{\boldsymbol{\Theta}} + \Delta \tag{24}$$

where $\tilde{\mathbf{w}} = \mathbf{w}^* - \hat{\mathbf{w}}$ and $\tilde{\boldsymbol{\Theta}} = \boldsymbol{\Theta}^* - \hat{\boldsymbol{\Theta}}$. In the following, some tuning laws will be derived to online tune the parameters of FCMAC to achieve favorable estimation of u^*. To

achieve this goal, the Taylor expansion linearization technique is employed to transform the nonlinear function into a partially linear form, that is

$$\tilde{\Theta} = \Theta_{\mathbf{m}}^T \tilde{\mathbf{m}} + \Theta_{\boldsymbol{\sigma}}^T \tilde{\boldsymbol{\sigma}} + \mathbf{h} \tag{25}$$

where $\tilde{\mathbf{m}} = \mathbf{m}^* - \hat{\mathbf{m}}$, $\tilde{\boldsymbol{\sigma}} = \boldsymbol{\sigma}^* - \hat{\boldsymbol{\sigma}}$, $\mathbf{h}$ is a vector of higher-order terms, $\Theta_{\mathbf{m}} = \left[\frac{\partial \Theta_{11}}{\partial \mathbf{m}} \cdots \frac{\partial \Theta_{jk}}{\partial \mathbf{m}} \cdots \frac{\partial \Theta_{n_j n_k}}{\partial \mathbf{m}}\right]|_{\mathbf{m}=\hat{\mathbf{m}}}$, $\Theta_{\boldsymbol{\sigma}} = \left[\frac{\partial \Theta_{11}}{\partial \boldsymbol{\sigma}} \cdots \frac{\partial \Theta_{jk}}{\partial \boldsymbol{\sigma}} \cdots \frac{\partial \Theta_{n_j n_k}}{\partial \boldsymbol{\sigma}}\right]|_{\boldsymbol{\sigma}=\hat{\boldsymbol{\sigma}}}$, and $\frac{\partial \Theta_{jk}}{\partial \mathbf{m}}$ and $\frac{\partial \Theta_{jk}}{\partial \boldsymbol{\sigma}}$ are defined as

$$\left[\frac{\partial \Theta_{jk}}{\partial \mathbf{m}}\right] = \left[\frac{\partial \Theta_{jk}}{\partial m_{111}}, \cdots, \frac{\partial \Theta_{jk}}{\partial m_{n_i n_j n_k}}\right]^T \tag{26}$$

$$\left[\frac{\partial \Theta_{jk}}{\partial \boldsymbol{\sigma}}\right] = \left[\frac{\partial \Theta_{jk}}{\partial \sigma_{111}}, \cdots, \frac{\partial \Theta_{jk}}{\partial \sigma_{n_i n_j n_k}}\right]^T. \tag{27}$$

Substitution of (25) into (24) yields

$$\begin{aligned} \tilde{u}_{FCMAC} &= \tilde{\mathbf{w}}^T \tilde{\Theta} + \hat{\mathbf{w}}^T (\Theta_{\mathbf{m}}^T \tilde{\mathbf{m}} + \Theta_{\boldsymbol{\sigma}}^T \tilde{\boldsymbol{\sigma}} + \mathbf{h}) + \tilde{\mathbf{w}}^T \hat{\Theta} + \Delta \\ &= \tilde{\mathbf{w}}^T \hat{\Theta} + \tilde{\mathbf{m}}^T \Theta_{\mathbf{m}} \hat{\mathbf{w}} + \tilde{\sigma}^T \Theta_{\sigma} \hat{\mathbf{w}} + \hat{\mathbf{w}}^T \mathbf{h} + \tilde{\mathbf{w}}^T \tilde{\Theta} + \Delta \end{aligned} \tag{28}$$

In order to speed up the parameter convergence of FCMAC, a PI-learning adaptation algorithm is employed to estimate the FCMAC's parameters [22]. The optimal vector $\mathbf{w}^*$ is decomposed into two parts as

$$\mathbf{w}^* = \eta_P \mathbf{w}_{\mathbf{P}}^* + \eta_I \mathbf{w}_{\mathbf{I}}^* \tag{29}$$

where η_P and η_I are positive constants, $\mathbf{w}_{\mathbf{I}}^* = \int_0^t \mathbf{w}_{\mathbf{P}}^* \, d\tau$, and $\mathbf{w}_{\mathbf{P}}^*$ and $\mathbf{w}_{\mathbf{I}}^*$ are the proportional and integral terms of $\mathbf{w}^*$, respectively. The estimation vector $\hat{\mathbf{w}}$ is decomposed into two parts as

$$\hat{\mathbf{w}} = \eta_P \hat{\mathbf{w}}_{\mathbf{P}} + \eta_I \hat{\mathbf{w}}_{\mathbf{I}} \tag{30}$$

where $\hat{\mathbf{w}}_{\mathbf{P}}$ and $\hat{\mathbf{w}}_{\mathbf{I}}$ are the proportional and integral terms of $\hat{\mathbf{w}}$, respectively, and $\hat{\mathbf{w}}_{\mathbf{I}} = \int_0^t \hat{\mathbf{w}}_{\mathbf{P}} \, d\tau$. Thus, $\tilde{\mathbf{w}}$ can be expressed as

$$\tilde{\mathbf{w}} = \eta_P \mathbf{w}_{\mathbf{P}}^* - \eta_P \hat{\mathbf{w}}_{\mathbf{P}} + \eta_I \tilde{\mathbf{w}}_{\mathbf{I}} \tag{31}$$

where $\tilde{\mathbf{w}}_{\mathbf{p}} = \mathbf{w}_{\mathbf{p}}^* - \hat{\mathbf{w}}_{\mathbf{p}}$. Substituting (31) into (28) yields

$$\begin{aligned} \tilde{u}_{FCMAC} &= (\eta_P \mathbf{w}_{\mathbf{P}}^* - \eta_P \hat{\mathbf{w}}_{\mathbf{P}} + \eta_I \tilde{\mathbf{w}}_{\mathbf{I}})^T \hat{\Theta} + \tilde{\mathbf{m}}^T \Theta_{\mathbf{m}} \hat{\mathbf{w}} + \tilde{\boldsymbol{\sigma}}^T \Theta_{\boldsymbol{\sigma}} \hat{\mathbf{w}} + \hat{\mathbf{w}}^T \mathbf{h} + \tilde{\mathbf{w}}^T \tilde{\Theta} + \Delta \\ &= \eta_I \tilde{\mathbf{w}}_{\mathbf{I}}^T \hat{\Theta} - \eta_P \hat{\mathbf{w}}_{\mathbf{P}}^T \hat{\Theta} + \tilde{\mathbf{m}}^T \Theta_{\mathbf{m}} \hat{\mathbf{w}} + \tilde{\boldsymbol{\sigma}}^T \Theta_{\boldsymbol{\sigma}} \hat{\mathbf{w}} + \varepsilon \end{aligned} \tag{32}$$

where the uncertain term $\varepsilon = \hat{\mathbf{w}}^T \mathbf{h} + \tilde{\mathbf{w}}^T \tilde{\Theta} + \eta_P \mathbf{w}_{\mathbf{P}}^{*T} \hat{\Theta} + \Delta$.

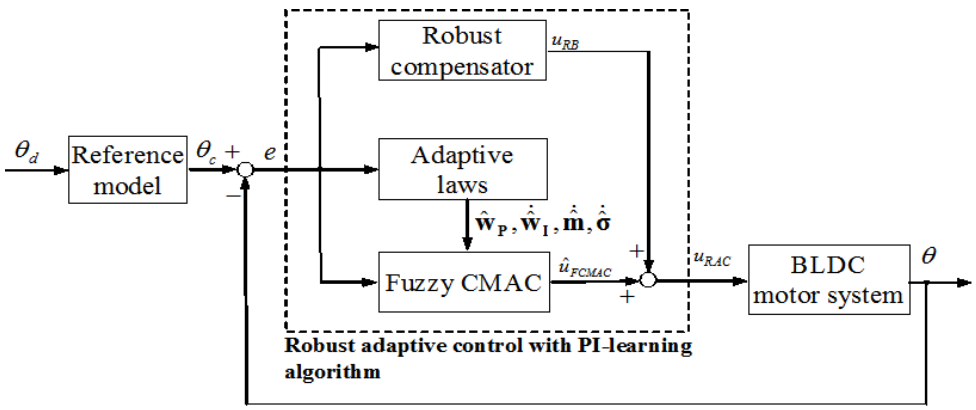

FIGURE 3. Robust adaptive control for BLDC motor system

4. **Design of Robust Adaptive Control System.** A robust adaptive control (RAC) system with adaptive learning laws is proposed as shown in Figure 3 to control a BLDC motor. The controller is assumed to take the following form

$$u_{RAC} = \hat{u}_{FCMAC} + u_{RB} \tag{33}$$

where $\hat{u}_{FCMAC}$ is an adaptive FCMAC that mimics the ideal controller, and u_{RB} is the robust controller designed to achieve robust tracking performance with the desired attenuation level. Substituting (33) into (10) and using (12) and (32) yield the error dynamic equation as

$$\begin{aligned} \dot{\mathbf{e}} &= \mathbf{\Lambda e} + \mathbf{b}(u^* - \hat{u}_{FCMAC} - u_{RB}) \\ &= \mathbf{\Lambda e} + \mathbf{b}(\eta_I \tilde{\mathbf{w}}_\mathbf{I}^T \hat{\mathbf{\Theta}} - \eta_P \hat{\mathbf{w}}_\mathbf{P}^T \hat{\mathbf{\Theta}} + \tilde{\mathbf{m}}^T \mathbf{\Theta_m} \hat{\mathbf{w}} + \tilde{\boldsymbol{\sigma}}^T \mathbf{\Theta}_{\boldsymbol{\sigma}} \hat{\mathbf{w}} + \varepsilon - u_{RB}) \end{aligned} \tag{34}$$

where $\mathbf{b} = \begin{bmatrix} 0 & g \end{bmatrix}^T$. In case of the existence of ε, consider a specified L_2 tracking performance [23]

$$\int_0^\tau \mathbf{e}^T \mathbf{Q} \mathbf{e} dt \le \mathbf{e}^T(0)\mathbf{P}\mathbf{e}(0) + \eta_I \tilde{\mathbf{w}}_\mathbf{I}^T(0)\tilde{\mathbf{w}}_\mathbf{I}(0) + \frac{1}{\eta_m}\tilde{\mathbf{m}}^T(0)\tilde{\mathbf{m}}(0) + \frac{1}{\eta_\sigma}\tilde{\boldsymbol{\sigma}}^T(0)\tilde{\boldsymbol{\sigma}}(0) + \rho^2 \int_0^\tau \varepsilon^2 dt \tag{35}$$

where $\mathbf{Q}$ and $\mathbf{P}$ are symmetric positive definite matrices, η_m and η_σ are positive constants, and ρ is a prescribed attenuation level. If the system starts with initial conditions $\mathbf{e}(0) = 0$, $\tilde{\mathbf{w}}_\mathbf{I}(0) = 0$, $\tilde{\mathbf{m}}(0) = 0$ and $\tilde{\sigma}(0) = 0$, the L_2 tracking performance in (35) can be rewritten as

$$\sup_{\varepsilon \in L_2[0,\tau]} \frac{\| \mathbf{e} \|}{\| \varepsilon \|} \le \rho \tag{36}$$

where $\| \mathbf{e} \|^2 = \int_0^\tau \mathbf{e}^T \mathbf{Q} \mathbf{e} dt$ and $\| \varepsilon \|^2 = \int_0^\tau \varepsilon^2 dt$. The attenuation constant ρ can be specified by the designer to achieve the desired attenuation ratio between $||\mathbf{e}||$ and $||\varepsilon||$. To guarantee the stability of the RAC system, a Lyapunov function is defined as

$$V = \frac{1}{2}\mathbf{e}^T\mathbf{P}\mathbf{e} + \frac{\eta_I}{2}\tilde{\mathbf{w}}_\mathbf{I}^T\tilde{\mathbf{w}}_\mathbf{I} + \frac{1}{2\eta_m}\tilde{\mathbf{m}}^T\tilde{\mathbf{m}} + \frac{1}{2\eta_\sigma}\tilde{\boldsymbol{\sigma}}^T\tilde{\boldsymbol{\sigma}}. \tag{37}$$

and a Riccati-like equation is defined as

$$\mathbf{\Lambda}^T\mathbf{P} + \mathbf{P}^T\mathbf{\Lambda} + \mathbf{Q} - \frac{2}{\delta}\mathbf{P}\mathbf{b}\mathbf{b}^T\mathbf{P} + \frac{1}{\rho^2}\mathbf{P}\mathbf{b}\mathbf{b}^T\mathbf{P} = 0. \tag{38}$$

Taking the derivative of Lyapunov function (37) and using (34) yields

$$\begin{aligned} \dot{V} &= \frac{1}{2}\dot{\mathbf{e}}^T\mathbf{P}\mathbf{e} + \frac{1}{2}\mathbf{e}^T\mathbf{P}\dot{\mathbf{e}} + \eta_I\tilde{\mathbf{w}}_\mathbf{I}^T\dot{\tilde{\mathbf{w}}}_\mathbf{I} + \frac{1}{\eta_m}\tilde{\mathbf{m}}^T\dot{\tilde{\mathbf{m}}} + \frac{1}{\eta_\sigma}\tilde{\boldsymbol{\sigma}}^T\dot{\tilde{\boldsymbol{\sigma}}} \\ &= \frac{1}{2}\mathbf{e}^T(\mathbf{\Lambda}^T\mathbf{P} + \mathbf{P}^T\mathbf{\Lambda})\mathbf{e} + \mathbf{e}^T\mathbf{P}\mathbf{b}(\eta_I\tilde{\mathbf{w}}_\mathbf{I}^T\hat{\mathbf{\Theta}} - \eta_P\hat{\mathbf{w}}_\mathbf{P}^T\hat{\mathbf{\Theta}} \\ &\quad + \tilde{\mathbf{m}}^T\mathbf{\Theta_m}\hat{\mathbf{w}} + \tilde{\boldsymbol{\sigma}}^T\mathbf{\Theta}_{\boldsymbol{\sigma}}\hat{\mathbf{w}} + \varepsilon - u_{RB}) - \eta_I\tilde{\mathbf{w}}_\mathbf{I}^T\dot{\hat{\mathbf{w}}}_\mathbf{I} - \frac{1}{\eta_m}\tilde{\mathbf{m}}^T\dot{\hat{\mathbf{m}}} - \frac{1}{\eta_\sigma}\tilde{\boldsymbol{\sigma}}^T\dot{\hat{\boldsymbol{\sigma}}} \\ &= \frac{1}{2}\mathbf{e}^T(\mathbf{\Lambda}^T\mathbf{P} + \mathbf{P}^T\mathbf{\Lambda})\mathbf{e} + \tilde{\mathbf{w}}_\mathbf{I}^T(\eta_I\mathbf{e}^T\mathbf{P}\mathbf{b}\hat{\mathbf{\Theta}} - \eta_I\dot{\hat{\mathbf{w}}}_\mathbf{I}) \\ &\quad + \tilde{\mathbf{m}}^T(\mathbf{e}^T\mathbf{P}\mathbf{b}\mathbf{\Theta_m}\hat{\mathbf{w}} - \frac{\dot{\hat{\mathbf{m}}}}{\eta_m}) + \tilde{\boldsymbol{\sigma}}^T(\mathbf{e}^T\mathbf{P}\mathbf{b}\mathbf{\Theta}_{\boldsymbol{\sigma}}\hat{\mathbf{w}} - \frac{\dot{\hat{\boldsymbol{\sigma}}}}{\eta_\sigma}) \\ &\quad - \eta_P\hat{\mathbf{w}}_\mathbf{P}^T\mathbf{e}^T\mathbf{P}\mathbf{b}\hat{\mathbf{\Theta}} + \mathbf{e}^T\mathbf{P}\mathbf{b}(\varepsilon - u_{RB}) \end{aligned} \tag{39}$$

If the adaptation laws of FCMAC are chosen as

$$\hat{\mathbf{w}}_{\mathbf{P}} = \mathbf{e}^T\mathbf{P}\mathbf{b}\hat{\Theta} \tag{40}$$

$$\dot{\hat{\mathbf{w}}}_{\mathbf{I}} = \mathbf{e}^T\mathbf{P}\mathbf{b}\hat{\Theta} \tag{41}$$

$$\dot{\mathbf{m}} = \eta_m\mathbf{e}^{\mathbf{T}}\mathbf{P}\mathbf{b}\Theta_{\mathbf{m}}\hat{\mathbf{w}} \tag{42}$$

$$\dot{\hat{\boldsymbol{\sigma}}} = \eta_\sigma\mathbf{e}^{\mathbf{T}}\mathbf{P}\mathbf{b}\Theta_{\boldsymbol{\sigma}}\hat{\mathbf{w}} \tag{43}$$

then (39) can be obtained as

$$\begin{aligned}\dot{V} &= \frac{1}{2}\mathbf{e}^T(\boldsymbol{\Lambda}^T\mathbf{P} + \mathbf{P}^T\boldsymbol{\Lambda})\mathbf{e} - \eta_P\hat{\mathbf{w}}_{\mathbf{P}}^T\hat{\mathbf{w}}_{\mathbf{P}} + \mathbf{e}^T\mathbf{P}\mathbf{b}(\varepsilon - u_{RB}) \\ &\le \frac{1}{2}\mathbf{e}^T(\boldsymbol{\Lambda}^T\mathbf{P} + \mathbf{P}^T\boldsymbol{\Lambda})\mathbf{e} + \mathbf{e}^T\mathbf{P}\mathbf{b}(\varepsilon - u_{RB}).\end{aligned} \tag{44}$$

If the robust controller is chosen as

$$u_{RB} = \frac{1}{\delta}\mathbf{b}^T\mathbf{P}\mathbf{e} \tag{45}$$

and using the Riccati-like Equation (38), then (44) can be obtained as

$$\begin{aligned}\dot{V} &\le \frac{1}{2}\mathbf{e}^T\left(-\mathbf{Q} + \frac{2}{\delta}\mathbf{P}\mathbf{b}\mathbf{b}^T\mathbf{P} - \tfrac{1}{\rho^2}\mathbf{P}\mathbf{b}\mathbf{b}^T\mathbf{P}\right)\mathbf{e} + \mathbf{e}^T\mathbf{P}\mathbf{b}\varepsilon - \frac{1}{\delta}\mathbf{e}^T\mathbf{P}\mathbf{b}\mathbf{b}^T\mathbf{P}\mathbf{e} \\ &\le -\frac{1}{2}\mathbf{e}^T\mathbf{Q}\mathbf{e} - \frac{1}{2\rho^2}\mathbf{e}^T\mathbf{P}\mathbf{b}\mathbf{b}^T\mathbf{P}\mathbf{e} + \mathbf{e}^T\mathbf{P}\mathbf{b}\varepsilon \\ &= -\frac{1}{2}\mathbf{e}^T\mathbf{Q}\mathbf{e} - \frac{1}{2}\left(\frac{\mathbf{e}^T\mathbf{P}\mathbf{b}}{\rho} - \rho\varepsilon\right)^2 + \frac{1}{2}\rho^2\varepsilon^2 \\ &\le -\frac{1}{2}\mathbf{e}^T\mathbf{Q}\mathbf{e} + \frac{1}{2}\rho^2\varepsilon^2.\end{aligned} \tag{46}$$

Assume $\varepsilon \in L_2[0,\tau]$, $\forall t \in [0,\infty]$. Integrating (46) yields

$$V(\tau) - V(0) \le -\frac{1}{2}\int_0^\tau \mathbf{e}^T\mathbf{Q}\mathbf{e}dt + \frac{1}{2}\rho^2\int_0^\tau \varepsilon^2 dt. \tag{47}$$

Since $V(\tau) \ge 0$, (47) implies the following inequality

$$\frac{1}{2}\int_0^\tau \mathbf{e}^T\mathbf{Q}\mathbf{e}dt \le V(0) + \frac{1}{2}\rho^2\int_0^\tau \varepsilon^2 dt. \tag{48}$$

By using (37), (48) is equivalent to (35). Since $V(0)$ is finite, if the approximation error $\varepsilon \in L_2$, that is $\int_0^\tau \varepsilon^2 dt < \infty$, the RAC system is asymptotically stable with L_2 tracking performance in the Lyapunov sense.

5. **Experimental Results.** Field programmable gate array (FPGA) is a fast prototyping IC component, and this kind of IC incorporates the architecture of a gate array and programmability of a programmable logic device. This paper uses the Altera Stratix II series FPGA chip with 50-MHz clock frequency for hardware implementation. The FPGA implementation has the advantage including shorter development time, small size, low cost, fast system execution speed, and high flexibility.

The BLDC motor control system is made up of hardware program modules and software Nios II programming interface as shown in Figure 4(a). The BLDC motor control experimental system is shown in Figure 4(b). The hardware program modules include the frequency divider module, the position command generator module, the encoder counter module, the function generator module and the D/A signal controller module. The frequency divider module derives a suitable clock frequency for all modules according to the clock frequency of an external clock oscillator; the position command generator generates the position command corresponding with the reference model; the encoder counter

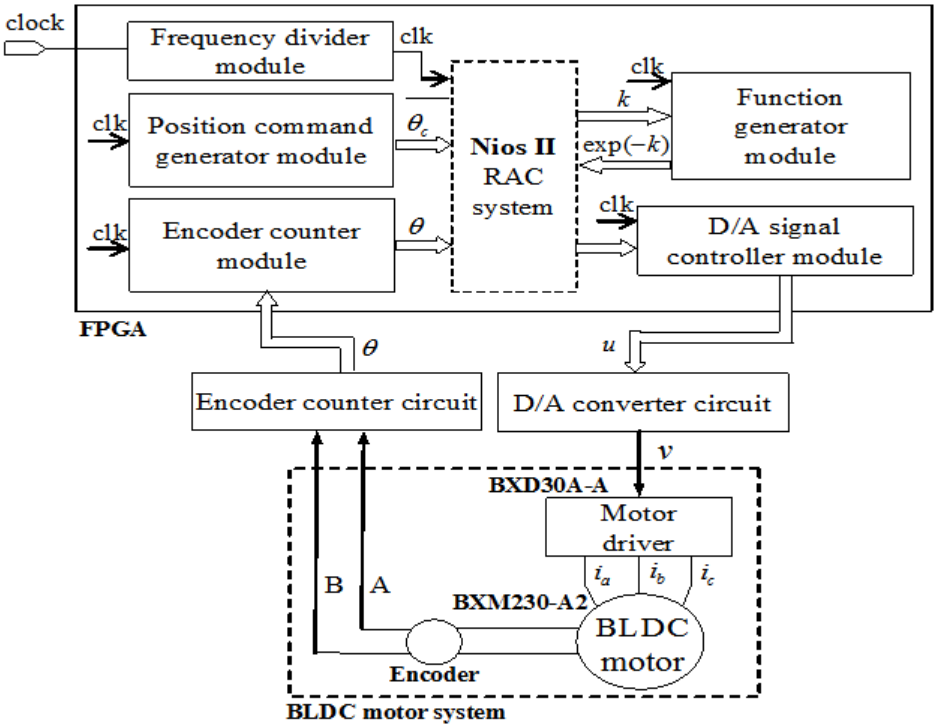

(a)

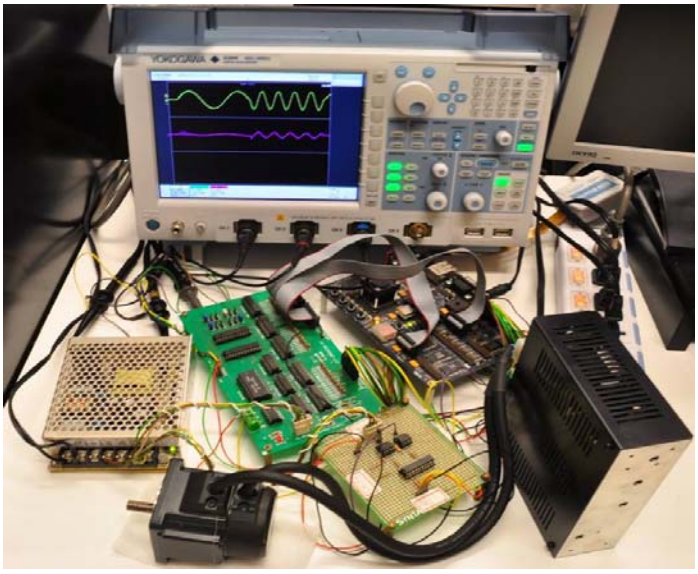

(b)

FIGURE 4. BLDC motor control experimental system setup

module uses the accumulator to increase the resolution of the rotor position; the function generator module uses the look-up table to produce the receptive-field function in (16); and the D/A signal controller module controls the external D/A converter circuit. The specifications of the adopted BLDC motor system manufactured by the Oriental Motor Company are outlined in Table 1. The external peripheral interfaces serve to transmit and receive the motor driver signals through a 12-bit encoder circuit and a 12-bit D/A converter circuit. The proposed control algorithm is realized in the Nios II kit. The software flowchart of the control algorithm is shown in Figure 5. In the main program, the controller parameters are initialized. Next, an interrupt interval for the interrupt service

routine with a 1-msec sampling rate is set. Then, the controller sampling time can be governed by the built-in timer, which generates periodic interruptions.

TABLE 1. The specifications of BLDC motor system

Output power HP (W)	1/25HP (30W)
Power supply	Single-phase 00 $\sim$ 115 VAC
Rated current	1.4 A
Gear/shaft type	Round Shaft
Variable speed range	30 $\sim$ 3000 r/min
Rated torque	0.1 N $\cdot$ m
Moment of inertia	$1.5 \cdot 10^{-4}$ kg $\cdot$ m^2
Load of inertia	$0.088 \cdot 10^{-4}$ kg $\cdot$ m^2
Components	BXD30A-A (Driver) BXM230-A2 (Motor)
Control detection system	Optimal encoder (500P/R)

In order to illustrate the effectiveness of the proposed design method, the proposed RAC is compared with an adaptive CMAC-based supervisory control [6] and a robust adaptive fuzzy control [19]. In the experiments, a second-order transfer function with 0.3-sec rise time is chosen as the reference model for the periodic step command

$$\frac{\omega_n^2}{s^2 + 2\xi\omega_n s + \omega_n^2} = \frac{400}{s^2 + 40s + 400} \tag{49}$$

where s is the Laplace operator, ξ is the damping ratio (set as one for critical damping) and ω_n is the un-damped natural frequency. In addition, when the command is a sinusoidal reference trajectory, the reference model is set as one. To demonstrat the tracking ability, the frequencies of the reference trajectories are changed at the fifth sec.

First, an adaptive CMAC-based supervisory controller proposed in [6] is employed to control the BLDC motor. The control parameters selected are $\eta_I = 2$, $\eta_m = \eta_\sigma = 0.2$. For a choice of $\mathbf{Q} = \mathbf{I}$, $k_1 = 2$ and $k_2 = 1$, and solving the Riccati-like Equation (38) with $2\rho^2 = \delta$ yields

$$\mathbf{P} = \begin{bmatrix} 1.7625 & 0.7812 \\ 0.7812 & 0.8088 \end{bmatrix}. \tag{50}$$

The adaptive CMAC-based supervisory controller requires information of approximation error bound E. The experimental results of the adaptive CMAC-based supervisory controller with $E = 0.5$ are shown in Figure 6. The tracking responses depicted in Figures 6(a) and 6(d), the associated control voltages depicted in Figures 6(b) and 6(e), and the tracking errors depicted in Figures 6(c) and 6(f) are triggered by a sinusoidal command and a periodic step command, respectively. Although favorable tracking responses can be obtained, the chattering phenomena of the control efforts shown in Figures 6(b) and 6(e) are undesirable in practical applications. The chattering phenomena in control efforts will wear the bearing mechanism and excite unstable system dynamics. Moreover, an adaptive CMAC-based supervisory controller with $E = 0.01$ is applied again. The experimental results with this small approximation error bound are shown in Figure 7. The tracking responses depicted in Figures 7(a) and 7(d), the associated control voltages depicted in Figures 7(b) and 7(e), and the tracking errors depicted in Figures 7(c) and 7(f) are triggered by a sinusoidal command and a periodic step command, respectively. As seen in Figures 7(a) and 7(d), the convergences of the tracking errors are slow at the beginning when the approximation error bound chosen is too small.

Next, a robust adaptive fuzzy controller proposed in [19] is applied to the BLDC motor control. The control parameters selected are $\eta_I = 2$, $\eta_m = \eta_\sigma = 0.2$. For a choice of $\mathbf{Q} = \mathbf{I}$, $k_1 = 2$, $k_2 = 1$ and different prescribed attenuation level for $\gamma = 0.8$ and $\gamma = 0.2$, the experimental results of robust adaptive fuzzy controller are shown in Figures 8 and 9, respectively. The experimental results reveal that although there are no chattering phenomena in the control efforts, the tracking errors cannot be eliminated appropriately.

Finally, the proposed RAC is also applied. The control parameters selected are $\eta_p = 0.02$, $\eta_I = 2$, $\eta_m = \eta_\sigma = 0.2$. For a choice of $\mathbf{Q} = \mathbf{I}$, $k_1 = 2$, $k_2 = 1$ and different prescribed attenuation levels for $\delta = 0.8$ and $\delta = 0.2$, the experimental results of the proposed RAC are shown in Figures 10 and 11, respectively. Comparing Figure 10 with Figures 6 and 8 and Figure 11 with Figures 7 and 9 show that the proposed RAC can much reduce the tracking error without control chattering at the expense of slightly larger

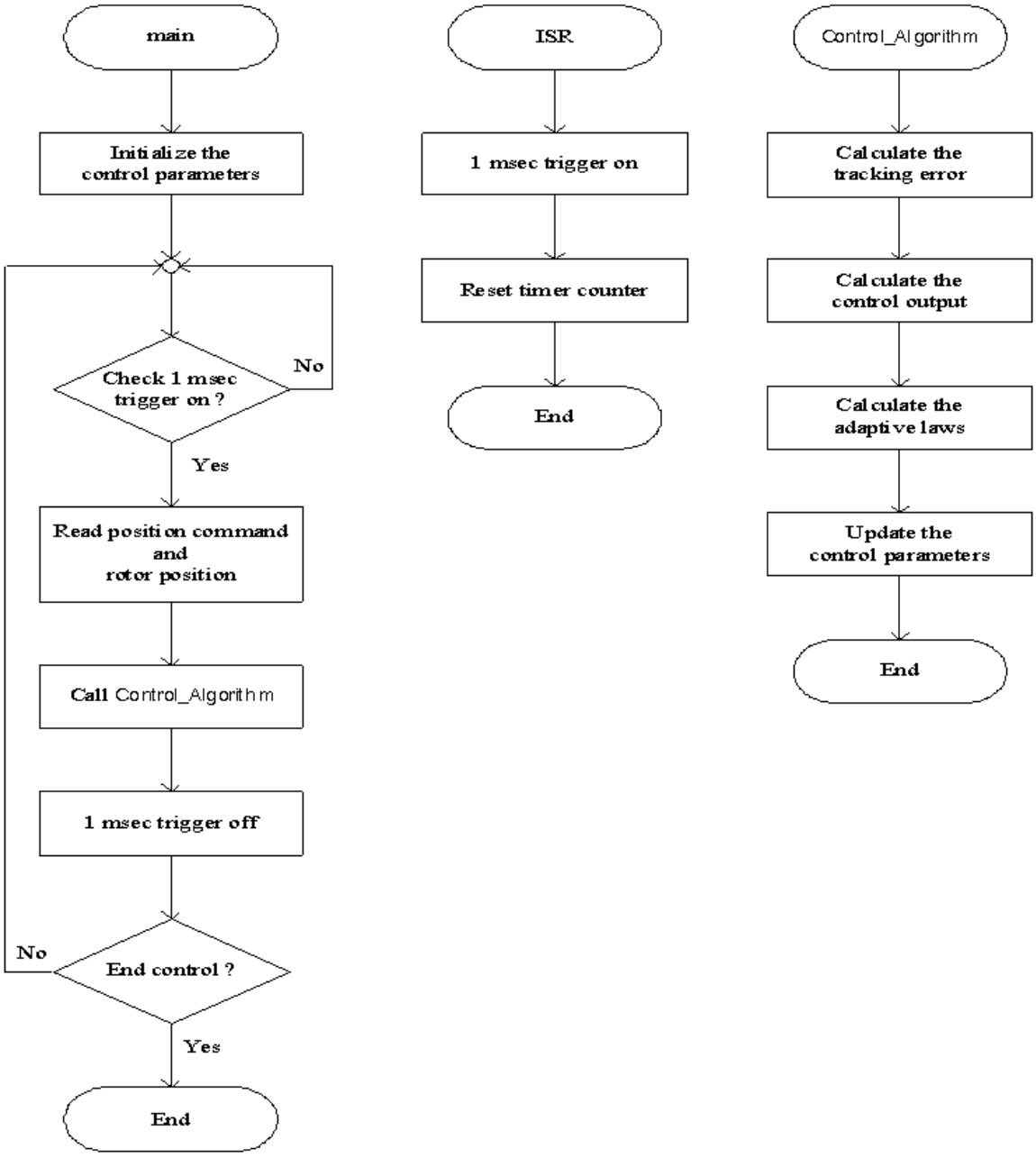

FIGURE 5. Flowchart of the software implement

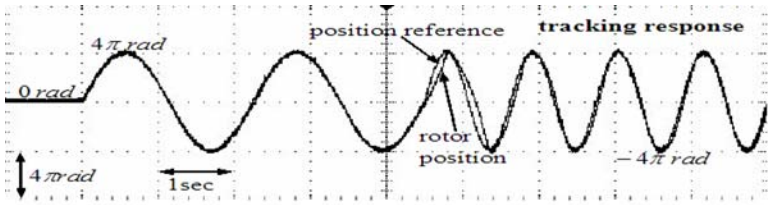

(a)

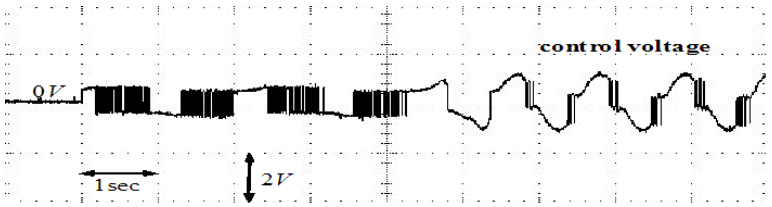

(b)

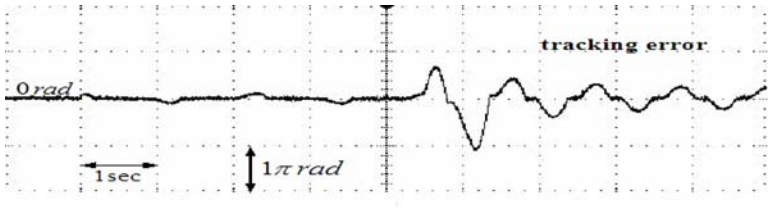

(c)

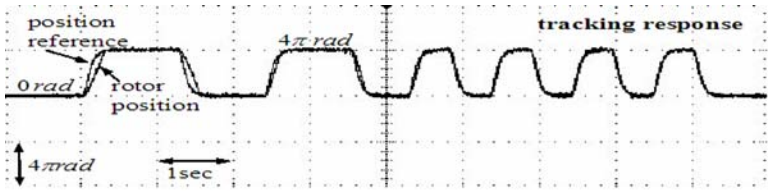

(d)

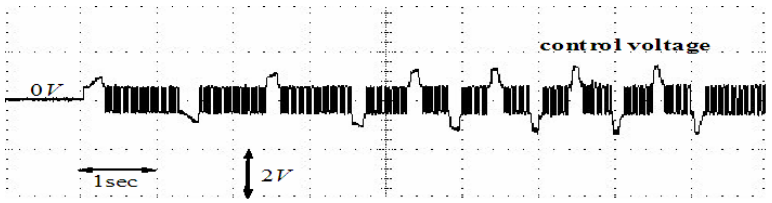

(e)

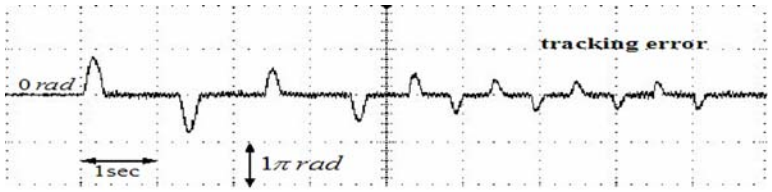

(f)

FIGURE 6. Experimental results of adaptive CMAC-based supervisory control with $E = 0.5$

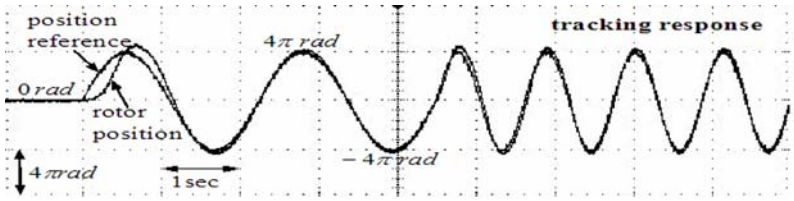

(a)

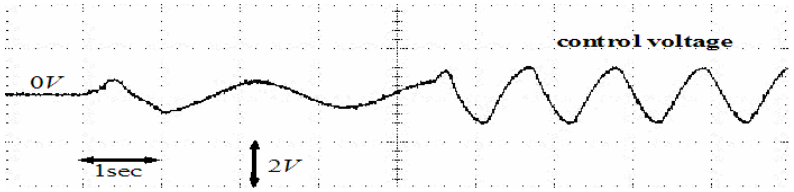

(b)

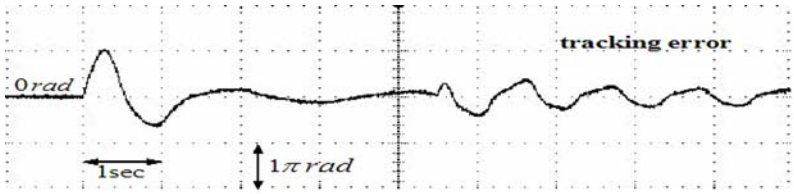

(c)

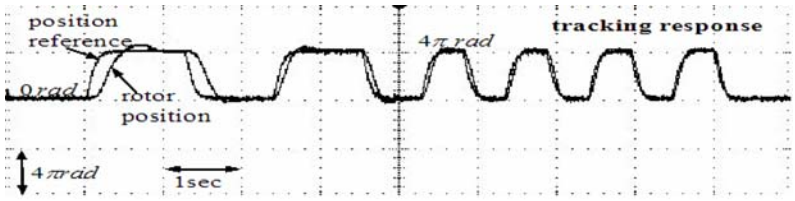

(d)

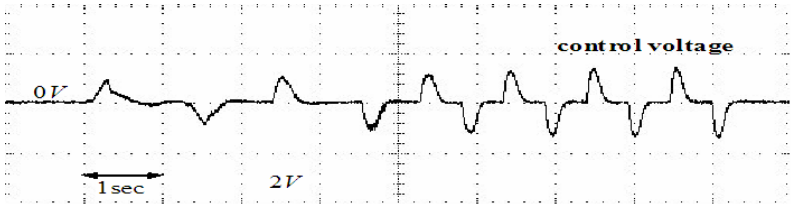

(e)

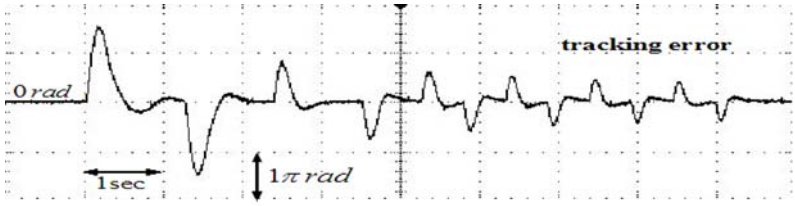

(f)

FIGURE 7. Experimental results of adaptive CMAC-based supervisory control with $E = 0.01$

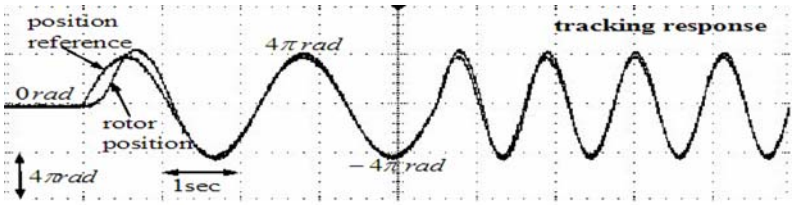

(a)

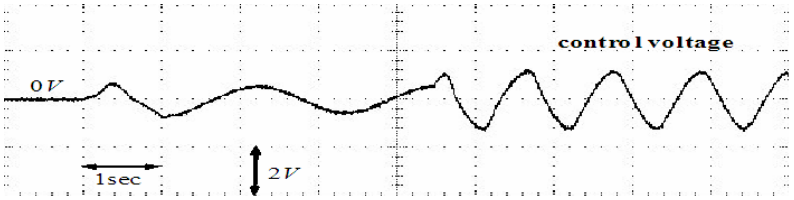

(b)

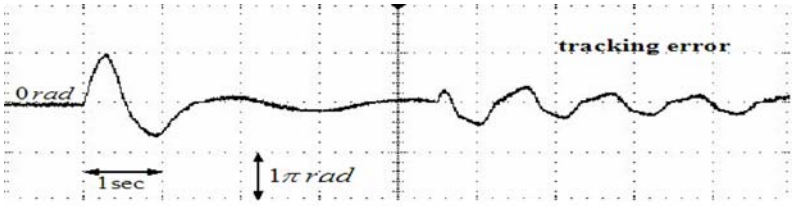

(c)

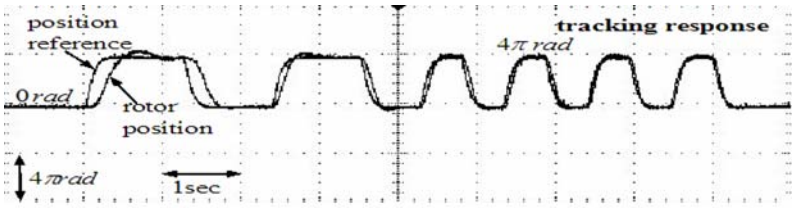

(d)

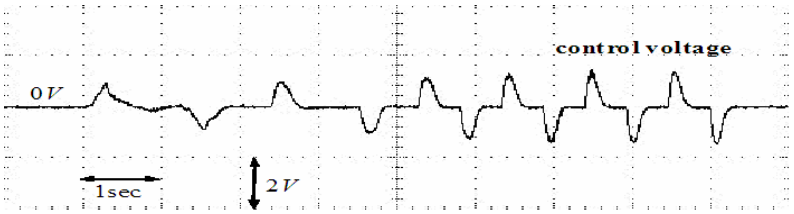

(e)

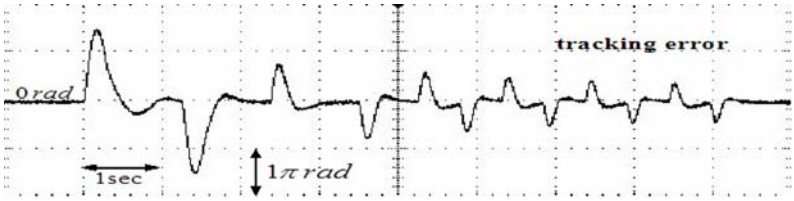

(f)

FIGURE 8. Experimental results of robust adaptive fuzzy controller with $\gamma = 0.8$

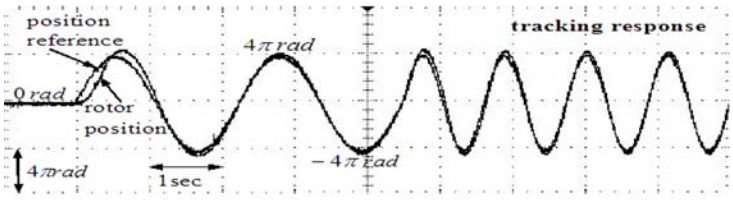

(a)

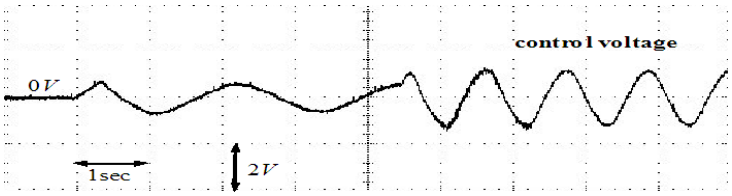

(b)

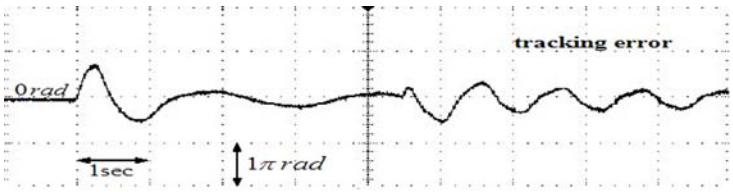

(c)

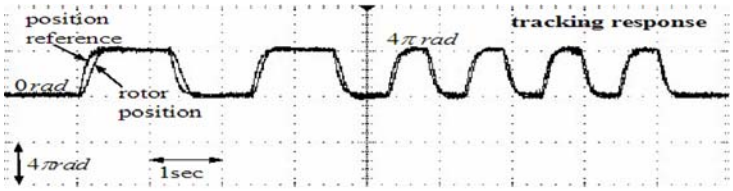

(d)

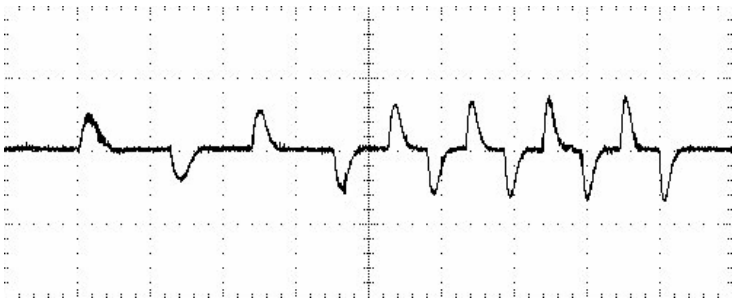

(e)

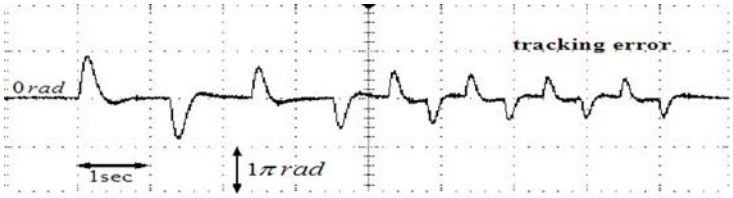

(f)

FIGURE 9. Experimental results of robust adaptive fuzzy controller with $\gamma = 0.2$

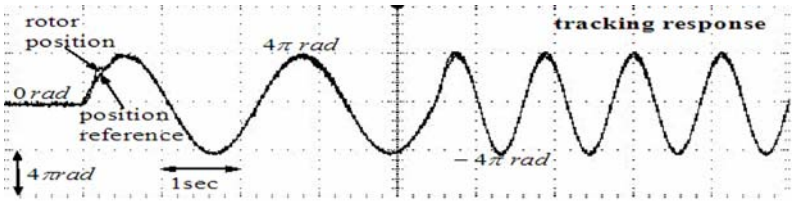

(a)

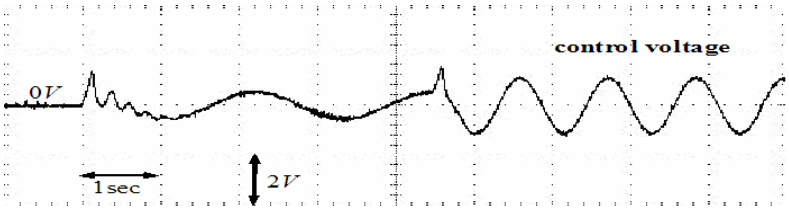

(b)

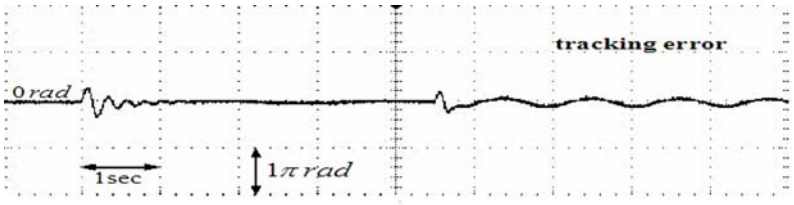

(c)

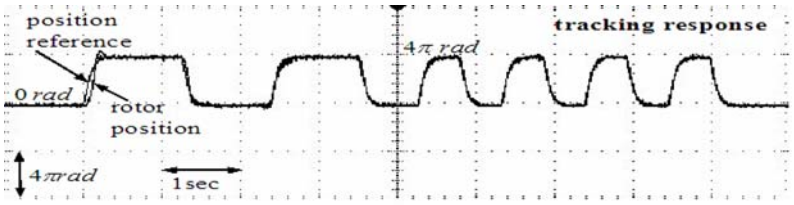

(d)

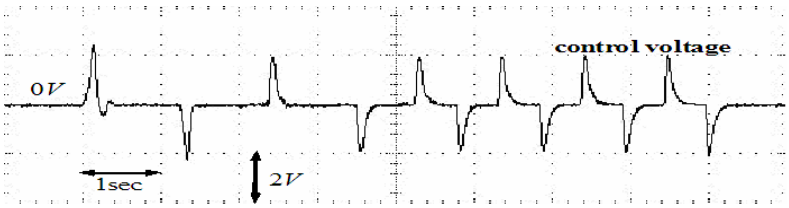

(e)

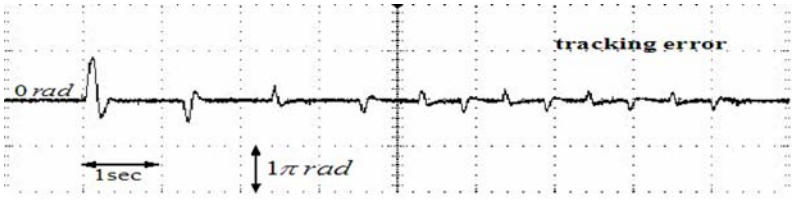

(f)

FIGURE 10. Experimental results of RAC with $\delta = 0.8$

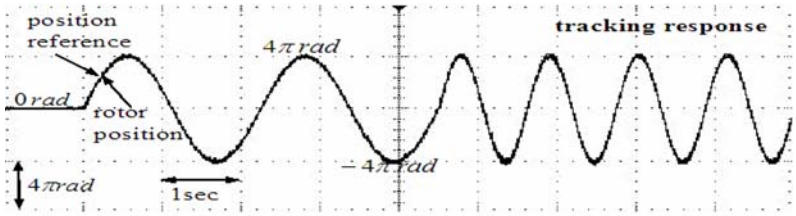

(a)

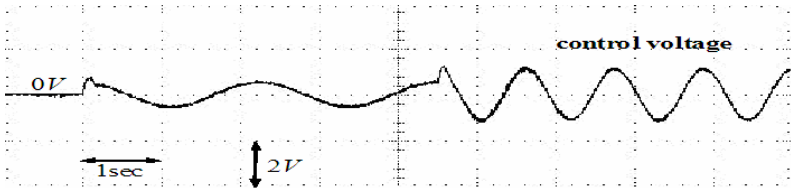

(b)

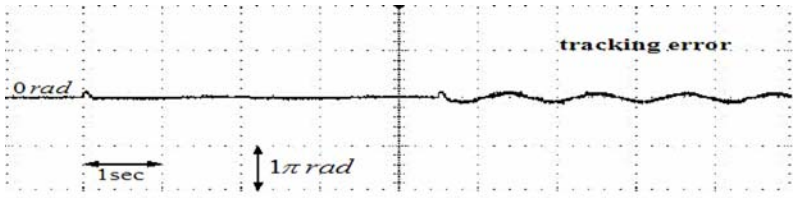

(c)

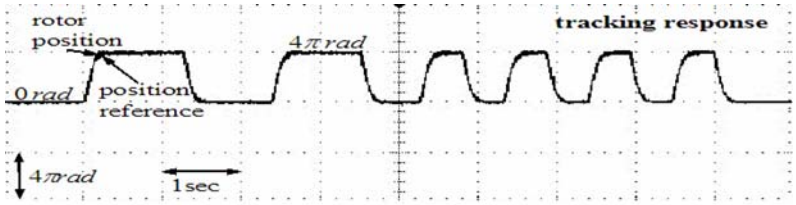

(d)

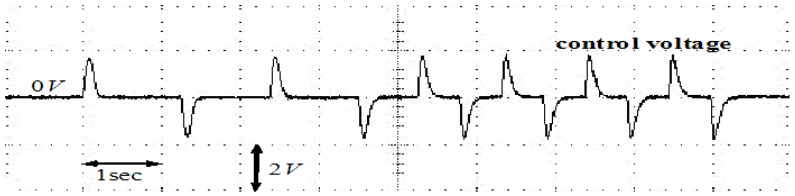

(e)

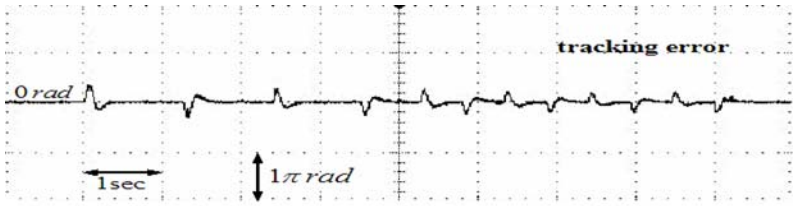

(f)

FIGURE 11. Experimental results of RAC with $\delta = 0.2$

control effort. This is reasonable by paying larger control effort to reduce the tracking error; and the slightly larger control effort is acceptable. Thus, the proposed RAC is best suitable for control of the BLDC motor than the other two control techniques. Moreover, comparing Figure 11(b) with Figure 10(b) and Figure 11(f) with Figure 10(f) show the tracking performance can be further improved as the attenuation level δ is set smaller. On summary, the proposed RAC method can achieve better tracking performance than the other control methods. The convergence of the tracking errors can be accelerated by the proposed control method.

6. **Conclusions.** A PI-learning fuzzy CMAC-based robust adaptive control (RAC) system has been successfully developed and implemented on a FPGA chip to control a BLDC motor. Implementing the control system using FPGA can achieve the characteristics of shorter development cycle, small size, low cost, fast execution speed and high flexibility. A comparison of control characteristics among adaptive CMAC-based supervisory controller, robust adaptive fuzzy controller and the proposed robust adaptive controller is demonstrated. The main contributions of this research are: (1) an RAC system is developed using a new PI-learning fuzzy CMAC; (2) a favorable tracking performance can be achieved by the proposed control method; and (3) a novel contribution in using FPGA to implement a fuzzy CMAC control system. In the proposed design method, the learning-rates of controller parameters should be determined through trial-and-error to achieve satisfactory performance. In future research, some optimization algorithms such as genetic algorithm or particle swarm optimization algorithm can be applied to auto-search the optimal learning-rates to further improve the parameter learning ability. Beside the BLDC motor, the developed theoretic results can be applied to most control systems such as other kinds of motor, robot, magnetic levitation system, and power converter.

Acknowledgments. The authors appreciate the reviewers' valuable comments and partial financial support from the National Science Council of Taiwan under grant NSC 96-2218-E-216-001.

REFERENCES

[1] J. Na, X. Ren, Y. Gao, G. Robert and C. C. Ramon, Adaptive neural network state predictor and tracking control for nonlinear time-delay systems, *International Journal of Innovative Computing, Information and Control*, vol.6, no.2, pp.627-639, 2010.

[2] R. Mei, Q.-X. Wu and C.-S. Jiang, Neural network robust adaptive control for a class of time delay uncertain nonlinear systems, *International Journal of Innovative Computing, Information and Control*, vol.6, no.3(A), pp.931-940, 2010.

[3] Y. Du, Q. Wu, C. Jiang and Y. Wang, Adaptive robust predictive control for hypersonic vehicles using recurrent functional link artificial neural network, *International Journal of Innovative Computing, Information and Control*, vol.6, no.12, pp.5351-5365, 2010.

[4] L. Yu, S. Fei, H. Zu and X. Li, Direct adaptive neural control with sliding mode method for a class of uncertain switched nonlinear systems, *International Journal of Innovative Computing, Information and Control*, vol.6, no.12, pp.5609-5618, 2010.

[5] J. C. Jan and S.-L. Hung, High-order MS CMAC neural network, *IEEE Trans. on Neural Network*, vol.12, no.3, pp.598-603, 2001.

[6] C.-M. Lin and Y.-F. Peng, Adaptive CMAC-based supervisory control for uncertain nonlinear systems, *IEEE Trans. on Systems, Man, Cybernetics, Part B: Cybernetics*, vol.34, no.2, pp.1248-1260, 2004.

[7] P.-L. Chang, Y.-K. Yang, H.-L. Shieh, F.-H. Hsieh and M.-D. Jeng, Grey relational analysis based approach for CMAC learning, *International Journal of Innovative Computing, Information and Control*, vol.6, no.9, pp.4001-4018, 2010.

[8] C.-M. Lin and T.-Y. Chen, Self-organizing CMAC control for a class of MIMO uncertain nonlinear systems, *IEEE Trans. on Neural Networks*, vol.20, no.9, pp.1377-1384, 2009.

[9] C.-H. Chen, C.-M. Lin and T.-Y. Chen, Intelligent adaptive control for MIMO uncertain nonlinear systems, *Expert Systems with Applications*, vol.35, no.3, pp.865-877, 2008.

[10] C. M. Lin, L. Y. Chen and C. H. Chen, RCMAC hybrid control for MIMO uncertain nonlinear systems using sliding-mode technology, *IEEE Trans. on Neural Networks*, vol.18, no.30, pp.708-720, 2007.

[11] S. F. Su, Z. J. Lee and Y. P. Wang, Robust and fast learning for fuzzy cerebellar model articulation controllers, *IEEE Trans. on Systems, Man, Cybernetics, Part B: Cybernetics*, vol.36, no.1, pp.203-208, 2006.

[12] T. F. Wu, P. S. Tsai, F. R. Chang and S. L. Wang, Adaptive fuzzy CMAC control for a class of nonlinear systems with smooth compensation, *IEE Proc. of Control Theory and Applications*, vol.153, no.6, pp.647-657, 2006.

[13] S.-Y. Cho, C. W. Ting and C. Quek, Thermal facial pattern recognition for personal verification using fuzzy CMAC model, *International Journal of Innovative Computing, Information and Control*, vol.7, no.1, pp.203-222, 2011.

[14] J. S. Ko, J. H. Lee and M. J. Youn, Robust digital position control of brushless DC motor with adaptive load torque observer, *Proc. of IEE Conference on Electric Power Applications*, vol.141, no.2, pp.63-70, 1994.

[15] F. Rodriguez and A. Emadi, A novel digital control technique for brushless DC motor drives, *IEEE Trans. on Industrial Electronics*, vol.54, no.5, pp.2365-2373, 2007.

[16] A. Rubaai, D. Ricketts and M. D. Kankam, Development and implementation of an adaptive fuzzy-neural-network controller for brushless drives, *IEEE Trans. on Industry Applications*, vol.38, no.2, pp.441-447, 2002.

[17] Z. Li and C. Xia, Speed control of brushless DC motor based on CMAC and PID controller, *The 6th World Congress on Intelligent Control and Automation*, vol.2, pp.6318-6322, 2006.

[18] A. Rubaai, A. R. Ofoli and D. Cobbinah, DSP-based real-time implementation of a hybrid H^{∞} adaptive fuzzy tracking controller for servo-motor drives, *IEEE Trans. on Industry Applications*, vol.43, no.2, pp.476-484, 2007.

[19] C.-M. Lin and C.-F. Hsu, Adaptive fuzzy sliding-mode control for induction servomotor systems, *IEEE Trans. on Energy Conversion*, vol.19, no.2, pp.362-368, 2004.

[20] Y. Liu, Z. Q. Zhu and D. Howe, Direct torque control of brushless DC drives with reduced torque ripple, *IEEE Trans. on Industry Applications*, vol.41, no.2, pp.599-608, 2005.

[21] L.-X. Wang, *Adaptive Fuzzy Systems and Control: Design and Stability Analysis*, Prentice-Hall, Englewood Cliffs, NJ, 1994.

[22] N. Golea, A. Golea and K. Benmahammed, Fuzzy model reference adaptive control, *IEEE Trans. on Fuzzy Systems*, vol.10, no.4, pp.436-444, 2002.

[23] W.-Y. Wang, M.-L. Chan, C. C. J. Hsu and T.-T. Lee, H^{∞} tracking-based sliding mode control for uncertain nonlinear systems via an adaptive fuzzy-neural approach, *IEEE Trans. on Systems, Man, Cybernetics, Part B: Cybernetics*, vol.32, no.4, pp.483-492, 2002.